environmental sciences proceedings

MDPI

Proceeding paper

Impact of Varied Conv-LSTM Model Parameters on Prediction Accuracy for NDSI-Based Salinity Index Analysis †

Hafssa Naciri [1,*], Nizar Ben Achhab [1], Naoufal Raissouni [2], Fatima Ezahrae Ezzaher [1]

[1] Mathematics and Intelligent Systems, Abdelmalek Essaâdi University, Tangier, Morocco; N.B.: nbenachhab@uae.ac.ma; F.E.: fatimazahra.ezzaher@etu.uae.ac.ma
[2] Remote Sensing, Systems and Telecommunications, Abdelmalek Essaâdi University, Tetouan, Morocco; N.R.: nraissouni@uae.ac.ma
* Correspondence: hafssa.naciri@etu.uae.ac.ma; Tel.: +212651138238
† Presented at the 5th International Electronic Conference on Remote Sensing, 7–21 Nov 2023, Available online: https://ecrs2023.sciforum.net/.

Abstract: In recent years, machine learning models have emerged as potent tools for prediction studies, particularly when dealing with sequential data. This research delves into the impact of Convolutional Long Short-Term Memory (Conv-LSTM) model parameters on the accuracy of predictions using Normalized Differential Salinity Index (NDSI-salinity) time series. Indeed, Landsat-8 satellite images of Tangier-Morocco collected between 2015 and 2022, have been used to compute NDSI-salinity time series dataset, forming the foundation for evaluating prediction accuracy. In this study, Conv-LSTM model was configured with three pivotal parameters: i) the number of "filters" in the main layer, ii) the number of "neurons" in the fully connected (dense) layer, and iii) the number of training "epochs". The NDSI-salinity time series data were employed to train and evaluate the model, with prediction accuracy assessed using the coefficient of determination (R^2) metric. The results uncover substantial insights into the relationship between Conv-LSTM model parameters and prediction accuracy for NDSI-salinity analysis. When considering a high number of epochs, the prediction accuracy remained relatively consistent at 97% across varying values of filters and neurons. In the context of medium number of epochs, the accuracy was influenced by the number of filters in the main layer. Specifically, when filters numbered between 10 and 100, accuracy remained below 60%. However, with a rise in filter count, accuracy exhibited an upward trend, ultimately plateauing at 96%. In contrast, for a low epochs count, the initial accuracy was negative. However, this was addressed by introducing an extensive number of filters in the main layer, reaching up to 10,000. The infusion of this high filter count yielded positive accuracy outcomes reaching more than 60%.

Keywords: Convolutional Long Short-Term Memory, Accuracy, Normalized Differential Salinity Index, Landsat-8

Citation: To be added by editorial staff during production.

Academic Editor: Firstname Lastname

Published: date

1. Introduction

Since the advent of data science with the appearance of deep learning, time series analysis has been employed to forecast and identify future patterns and trends along with monitoring and detecting land cover changes [1]. A wide range of models is utilized regarding time series forecasting, which includes statistical methods such as automatic regression models [2], and others based on machine learning methodologies such as Artificial Neural Network (ANN), Convolutional Neural Network (CNN), Recurrent Neural Network (RNN) [3], and Long Short-Term Memory Network (LSTM) [4].

Time series forecasting stands as an essential tool in modern data science and decision-making, having the ability to display valuable information from past data and guide to decisive actions for the future. Simultaneously, at the intersection of technology and

data, there is a remarkable increase in the capacity to enhance the accuracy of time series forecasting [5]. Thus, advanced machine learning categories, such as deep learning models, have contributed to improve forecasting accuracy, by enabling complicated patterns extraction from data sequences, even those with complex spatiotemporal dependencies. Moreover, combining geospatial information, drawn from satellites, with time series forecasting improves environmental, urban, and natural systems evolution understanding. This combination helps in addressing critical challenges, such as climate change monitoring, disaster prediction, and urban planning, with unprecedented precision.

This research examines the impact of Convolutional Long Short-Term Memory (Conv-LSTM) model parameters on prediction accuracy using Normalized Differential Salinity Index (NDSI-salinity) time series. In fact, Conv-LSTM model architecture constitutes an evolution of Long Short-Term Memory (LSTM) model, engineered to capture both spatial and temporal dependencies in sequences [6]. Unlike traditional LSTMs, Conv-LSTMs embrace spatial structure of input data by coupling LSTM units with convolutional layers. This synergistic design allows Conv-LSTM to extract and integrate features across both time and space, making them adept at analyzing complex time series data with spatial correlations, such as satellite images or environmental measurements. Accordingly, NDSI-salinity time series was constructed using Landsat-8 satellite imagery, covering Tangier region in Morocco from 2015 to 2022. Within each year, a set of four images corresponding to the different seasons (i.e., winter, spring, summer, and autumn) was systematically selected. Consequently, the computed NDSI-salinity time series was employed as input dataset in order to conduct a detailed evaluation of forecast accuracy when varying Conv-LSTM parameterization.

The upcoming section presents materials and methods, which include study area and utilized satellite data, as well as an introduction to NDSI-salinity index. Additionally, Conv-LSTM model configuration are presented, and parameter adjustment is explained. Next, the results are discussed, particularly in terms of forecasting accuracy comparison across three scenarios: low numbers of epochs, medium numbers of epochs, and high numbers of epochs.

2. Materials and Methods

2.1. Study Area

This research centers on ecologically diverse region of Tangier, located in northern Morocco in Tangier-Tetouan-Al Hoceima prefecture (Figure 1). Geographically, Tangier extends to 05°48′W in longitude and 35°46′N in latitude. Situated on west Mediterranean Sea and east Atlantic Ocean, this region presents a harmonious convergence of coastal, urban, and natural landscapes within its expansive 138.83 square kilometers. This region contains a variety of soil types. For instance, coastal areas of Tangier predominantly feature sandy soils, while soils encircling Rif mountains, with their diverse elevations, exhibit varying compositions. Additionally, urban soils, shaped by the forces of urbanization and construction activities, display various characteristics depending upon different construction materials and land utilization.

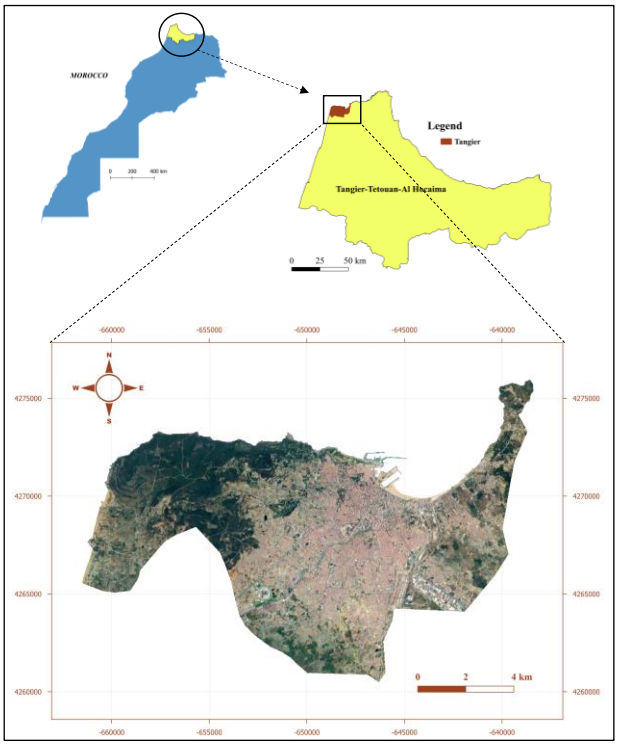

Figure 1. Situation map of the study area.

2.2. Data collection

The used data was collected from Landsat-8 satellite, launched by NASA in order to extends the legacy of Earth observation missions initiated by previous Landsat satellites. This initiative has resulted in the accumulation of an extensive satellite imagery repository, widely employed in diverse and influential studies across various domains. In this research, Landsat-8 Collection 2 (C2) Level 2 Science Products (L2SP) data were utilized (Table 1), with level-3 processing, involving calibration and atmospheric correction procedures executed using the Land Surface Reflectance Code (LaRSC) algorithm. Access to the product dataset is available via the USGS Earthdata platform [7].

Table 1. Landsat-8 spectral band characteristics used in this study.

Band number	Name	Wavelength (μm)	Spectral resolution (m)	Temporal resolution
Band4	Red	0.64-0.67	30	16 days
Band5	Near Infrared	0.85-0.88		

In this study, four images for each year were selected, each representing one of the four seasons (Winter, Spring, Summer, and Autumn) (Table 2).

Table 2. Image dates of Landsat-8 satellite used in the analysis of studied region.

Seasons	Image dates (dd/mm/yy)							
Winter	03/01/15	31/01/16	17/01/17	11/01/18	07/01/19	01/01/20	12/01/21	06/01/22
Spring	02/04/15	27/04/16	07/04/17	17/04/18	13/04/19	01/05/20	18/04/21	06/05/22
Summer	07/07/15	09/07/16	19/07/17	06/07/18	18/07/19	04/07/20	07/07/21	10/07/22
Autumn	09/09/15	27/09/16	30/09/17	24/09/18	27/09/19	22/09/20	02/10/21	27/09/22

2.3. Normalized Differential Salinity Index (NDSI-salinity)

The NDSI-salinity for soil salinity [8], is an index used to estimate soil salinity levels using remote sensing data, typically satellite imagery. The primary purpose of NDSI-salinity for soil salinity is to monitor and assess soil salinity levels over large areas. High soil salinity can be detrimental to plant growth, affecting crop yields and soil quality. Therefore, this index is widely used in agricultural management and environmental studies to identify areas where soil salinity may be a concern. The NDSI-salinity index is calculated using Red and Near-Infrared reflectance [9].

$$NDSI_{salinity} = (Band4-Band5) / (Band4+Band5) \quad (1)$$

After computing NDSI-based salinity index using the aforementioned formula, we derived an average NDSI-salinity value from each image, and subsequently we constructed a time series. Figure 2 provided in this study illustrates the temporal variation of these average NDSI-salinity values from 2015 to 2022.

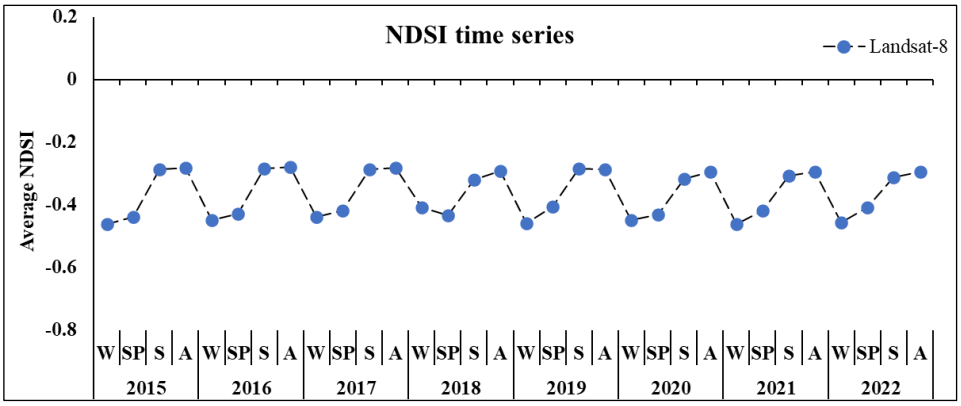

Figure 2. Temporal variation of average NDSI-salinity. W: Winter, Sp: Spring, S: Summer, and A: Autumn.

2.4. Methodology

2.4.1. Conv-LSTM Model Configuration

The model was developed using essential Python libraries, including NumPy [10], Pandas [11], and Keras [12]. To begin, the average NDSI-salinity time series data for forecasting was imported using the Pandas library. Then, data preprocessing was conducted, involving data cleaning and normalization. Following this preprocessing step, the data was divided into training and testing sets, using 60% of dataset for model training and the remaining 40% for model testing. Typically, the training set is utilized to train the Conv-LSTM model, while the testing set is employed to assess the model's performance. The Conv-LSTM model was constructed using the Keras library, consisting of two layers. Each layer is defined by the number of filters in the main layer and the number of neurons in the fully connected (dense) layer. For model compilation, the Mean Squared Error (MSE) was chosen as the loss function, and the "adam" optimizer was applied. During the training of the Conv-LSTM model, specifying the number of training epochs was a crucial step. Finally, the performance of the Conv-LSTM model was assessed using the coefficient of determination (R^2) (Figure 3). The formula for computing R^2 involves comparing the actual values in the test dataset with the predicted values generated by our model.

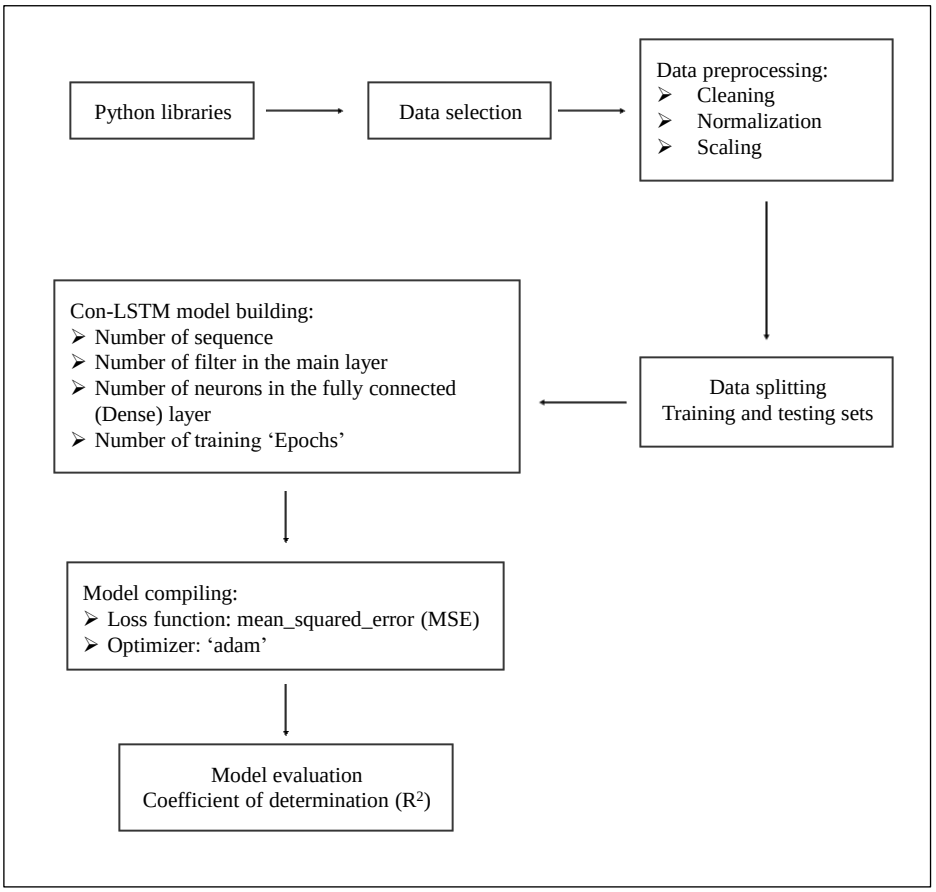

Figure 3. Conv-LSTM flowchart.

2.4.2. Parametrization of Conv-LSTM

To analyze the impact of critical parameters on the performance of the Conv-LSTM model and its predictive accuracy, we configured the model using three key parameters. First, the number of filters in the main layer was manipulated to assess its influence on the model ability to capture temporal patterns and spatial features. The filter count was systematically varied, ranging from 10 to 100 with increments of 10, and from 100 to 1000 with increments of 100. Next, the number of neurons in the fully connected (dense) layer was held constant at a range of 10 to 100 neurons. Finally, we investigated the role of the number of training epochs, which dictates the number of iterations the model undergoes while learning from the dataset. This parameter was varied across three values: 10, 50, and 100, representing low, medium, and high numbers of epochs, respectively. These variations allowed us to explore the model performance under different training scenarios and ascertain how each parameter influenced the accuracy of predictions.

3. Results and Discussion

The results provide valuable insights into the interaction between Conv-LSTM model parameters and the accuracy of NDSI-salinity analysis. In scenarios where a high number of epochs (i.e., epochs=100) were employed (Figure 4a), prediction accuracy exhibited remarkable stability, consistently hovering around 97% regardless of variations in filter counts and neuron numbers. This stability suggests that, beyond a certain point, increasing the number of epochs yields diminishing returns in terms of accuracy enhancement. On the other hand, in cases with a medium number of epochs (i.e., epochs=50), the observed fluctuations in accuracy were more pronounced (Figure 4b). Notably, accuracy was influenced by the number of filters in the main layer. Specifically, when the filter count ranged between 10 and 100, accuracy levels remained below 60%. However, with an

escalation in the filter count, accuracy demonstrated a notable upward trajectory, ultimately reaching a plateau at 96%. Finally, when a low epoch count (i.e., epochs=10) was employed, the initial accuracy was in the negative range (Figure 4c). Nevertheless, this challenge was effectively addressed by introducing a substantial number of filters in the main layer, counting up to 10,000. This infusion of a high filter count yielded positive accuracy outcomes exceeding 60%. These findings underscore the compensatory effect of a substantial filter count in qualifying the limitations posed by a limited number of training epochs.

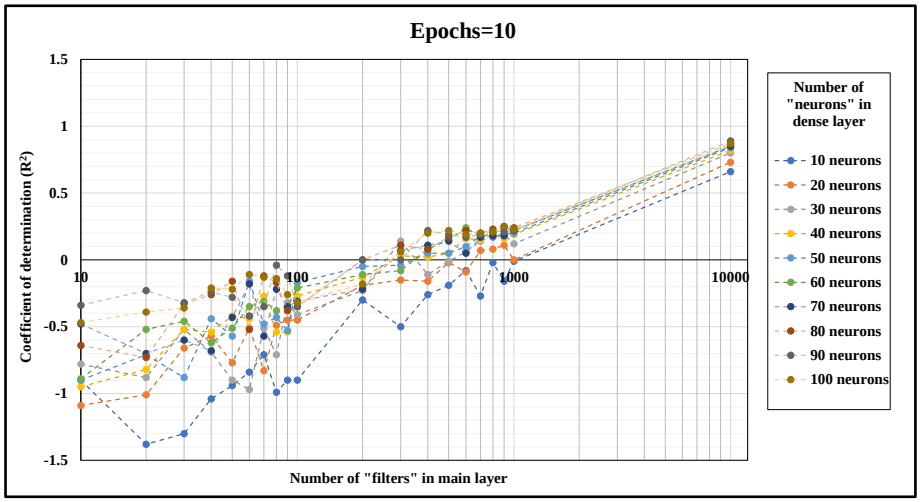

(**a**)

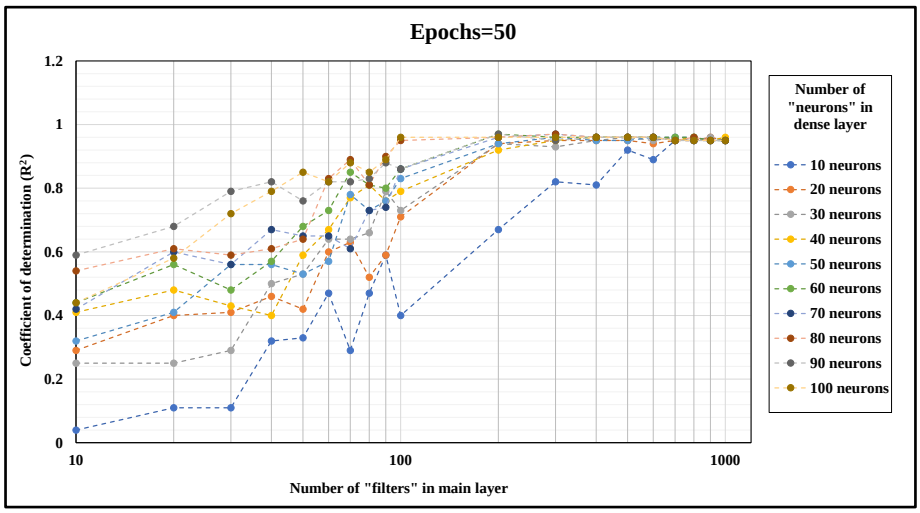

(**b**)

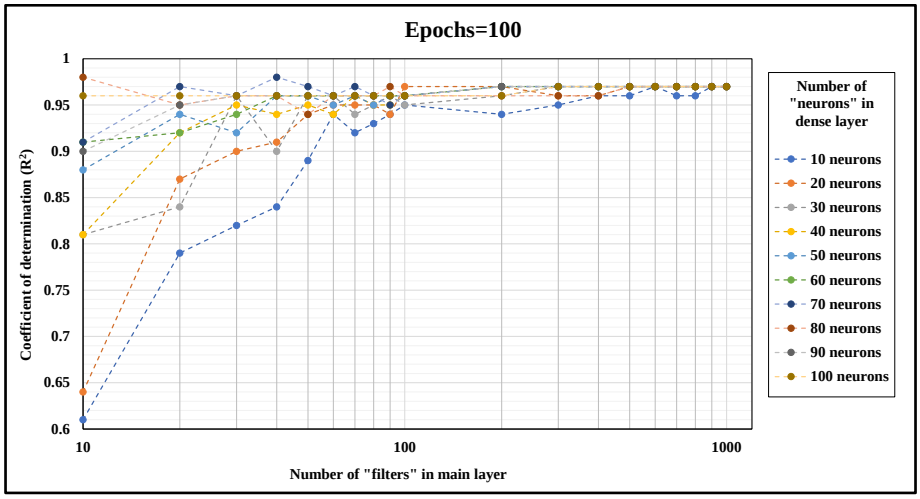

(**c**)

Figure 4. Forecasting accuracy variations in three scenarios: (**a**) low number of epochs, (**b**) medium number of epochs, (**c**) high number of epochs.

4. Conclusion

In this study, Convolutional Long Short-Term Memory (Conv-LSTM) model performance was explored in the context of NDSI-salinity analysis. Employing remote sensing data from Landsat-8, impact of three pivotal model parameters was studied: number of filters in the main layer, number of neurons in the fully connected (dense) layer, and number of training epochs. The findings of this research shed light on the relationship between these parameters and prediction accuracy. Under varying conditions, interesting dynamics in model accuracy were observed. As a result, forecasting accuracy showed an upward trend, although with different speed. The model rapidly reached saturation in 97% with a high number of epochs (equal to 100) and neurons in dense layer (from 80 to 100 neurons). On the other hand, achieving saturation in scenarios with a low number of epochs (equal to 10) necessitated a substantially higher filter count in main layer (equal to 10,000).

Author Contributions: Methodology, H.N., N.B., N.R., F.E.; formal analysis, H.N., N.B., N.R., F.E.; data curation, N.B.; writing—original draft preparation, H.N., F.E.; writing—review and editing, H.N., N.B., N.R., F.E.; supervision, N.B, N.R.; All authors have read and agreed to the published version of the manuscript.

Funding: This research received no external funding.

Institutional Review Board Statement: Not applicable.

Informed Consent Statement: Not applicable.

Data Availability Statement: Unavailability of data due to ethical restrictions.

Conflicts of Interest: The authors declare no conflict of interest.

References

1. Ferchichi, A.; Abbes, A.B.; Barra, V.; Farah, I.R. Forecasting Vegetation Indices from Spatio-Temporal Remotely Sensed Data Using Deep Learning-Based Approaches: A Systematic Literature Review. Ecological Informatics 2022, 68, 101552, doi:10.1016/j.ecoinf.2022.101552.
2. Hill, D.C.; McMillan, D.; Bell, K.R.W.; Infield, D. Application of Auto-Regressive Models to U.K. Wind Speed Data for Power System Impact Studies. IEEE Transactions on Sustainable Energy 2012, 3, 134–141, doi:10.1109/TSTE.2011.2163324.
3. Hüsken, M.; Stagge, P. Recurrent Neural Networks for Time Series Classification. Neurocomputing 2003, 50, 223–235, doi:10.1016/S0925-2312(01)00706-8.
4. Zaytar, M.A.; El Amrani, C. Sequence to Sequence Weather Forecasting with Long Short-Term Memory Recurrent Neural Networks. International Journal of Computer Applications 2016, 143, 7–11, doi:10.5120/ijca2016910497.
5. Naciri, H.; Ben Achhab, N.; Ezzaher, F.-E.; Sobrino, J.A.; Raissouni, N. Mediterranean Basin Vegetation Forecasting Approaches: Accuracy Analysis & Climate-Land Cover-Sensor Nexus Impacts. International Journal of Remote Sensing 2023, 1–20, doi:10.1080/01431161.2023.2217984.

6. Shi, X.; Chen, Z.; Wang, H.; Yeung, D.-Y.; Wong, W.; Woo, W. Convolutional LSTM Network: A Machine Learning Approach for Precipitation Nowcasting. In Proceedings of the Advances in Neural Information Processing Systems; Curran Associates, Inc., 2015; Vol. 28.
7. EarthExplorer Available online: https://earthexplorer.usgs.gov/ (accessed on 25 September 2023).
8. Ezzaher, F.-E.; Ben Achhab, N.; Naciri, H.; Sobrino, J.A.; Raissouni, N. Assessing 100 Biophysical Indices Performances in the Mediterranean Basin Using Multi-Satellite Data. International Journal of Remote Sensing 2023, 1–49, doi:10.1080/01431161.2023.2209917.
9. Barreto, A.C.; Ferreira Neto, M.; Oliveira, R.P. de; Moreira, L.C.J.; Medeiros, J.F. de; Sá, F.V. da S. Comparative Analysis of Spectral Indexes for Soil Salinity Mapping in Irrigated Areas in a Semi-Arid Region, Brazil. Journal of Arid Environments 2023, 209, 104888, doi:10.1016/j.jaridenv.2022.104888.
10. Van Der Walt, S.; Colbert, S.C.; Varoquaux, G. The NumPy Array: A Structure for Efficient Numerical Computation. Comput. Sci. Eng. 2011, 13, 22–30, doi:10.1109/MCSE.2011.37.
11. McKinney, W. Data Structures for Statistical Computing in Python.; Austin, Texas, 2010; pp. 56–61.
12. Manaswi, N.K. Understanding and Working with Keras. In Deep Learning with Applications Using Python : Chatbots and Face, Object, and Speech Recognition With TensorFlow and Keras; Manaswi, N.K., Ed.; Apress: Berkeley, CA, 2018; pp. 31–43 ISBN 978-1-4842-3516-4.